Mitigating the Bfl-1-mediated antiapoptotic pathway in diffuse large B cell lymphoma by inhibiting HDACs

Running title: Bfl-1 inhibition by HDAC inhibitor in DLBCL

Keywords: Diffuse Large B-cell lymphoma (DLBCL), Bfl-1, Histone Deacetylase (HDAC) inhibitor, Response prediction, biomarker, apoptosis

Eunchae Park[1, 2], Chansub Lee[1, 2], Jihyun Park[1, 2], Jun Liu[1, 2], Junshik Hong[1,2,4], Dong-Yeop Shin[1,2,4], Ja Min Byun[1,2,4], Hongseok Yun[2,3,4], Youngil Koh[1,2,4], and Sung-Soo Yoon[1,2,4]

[1]Cancer Research Institute, Seoul National University College of Medicine, Seoul, Republic of Korea.

[2]Center for Medical Innovation, Seoul National University Hospital, Seoul, Republic of Korea.

[3]Center for Precision Medicine, Seoul National University Hospital, Seoul, Republic of Korea.

[4]Division of Hematology and Medical Oncology, Department of Internal Medicine, Seoul National University Hospital, Seoul, Republic of Korea

Corresponding authors

Sung-Soo Yoon, M.D., Ph.D.

Professor

Division of Hematology and Medical Oncology, Seoul National University Hospital, 101, Daehak-ro, Jongno-gu, Seoul 03082, Republic of Korea

Tel: +82-2-2072-3079, Fax: +82-2-762-9662

E-mail: ssysmc@snu.ac.kr

Youngil Koh, M.D., Ph.D.

Associate Professor Division of Hematology and Medical Oncology, Seoul National University Hospital, 101, Daehak-ro, Jongno-gu, Seoul 03080, Republic of Korea

Tel: +82-2-2072-7217, Fax: +82-2-2072-7379

E-mail: go01@snu.ac.kr

Text word count: 2996 / 4000

Abstract word count: 191 / 250

Figure/table count: 6 / 0

Supplemental material: 11 supplemental figures, 5 supplemental tables

Reference count: 38

Key points:

- Diffuse large B cell lymphoma shows apoptosis to HDAC inhibitors depending on the Bfl-1 expression level.
- Effect of HDAC inhibitors in diffuse large B-cell lymphoma with high Bfl-1 is mediated via Noxa and Wt-1 with HDAC class-specificity.

Abstract

Endogenous Bfl-1 expression renders diffuse large B-cell lymphoma (DLBCL) cells insensitive to Bcl-2 and/or Mcl-1 inhibitors. Considering the difficulties of developing a direct Bfl-1 inhibitor, we intended to inhibit histone deacetylase (HDAC) to mitigate the adverse biologic role of Bfl-1 by modulating Wt-1 and Noxa. In vitro assays including western blotting, qRT-PCR, proliferation assay, and flow cytometry were performed using DLBCL cell lines. shRNA-mediated Bfl-1 knockdown DLBCL cells were generated to verify the role of Bfl-1 in HDAC inhibitors sensitivity. DLBCL cells expressing high Bfl-1 exhibited enhanced sensitivity to pan-HDAC inhibitor panobinostat compared to low Bfl-1 expressing cells, mainly attributable to the difference in the amount of apoptosis. HDAC inhibitors decreased Bfl-1 and Wt-1 expressions while increased Noxa level in DLBCL, as we hypothesized. The Bfl-1 knockdown experiment demonstrated that HDAC inhibitor's sensitivity depends on the expression level of Bfl-1 in DLBCL cells. Furthermore, we found the specific HDAC class was expected to play a critical role in Bfl-1 inhibition by comparing the results of several HDAC inhibitors. In summary, our study provides a rationale for using HDAC inhibitors to induce apoptosis in DLBCL patients using Bfl-1 as a predictive biomarker.

Introduction

Diffuse large B-cell lymphoma (DLBCL) is a B-cell lymphoma constituting ~40% of non-Hodgkin B-cell lymphomas.[1] DLBCL is genetically heterogeneous with various subtypes according to genetic irregularities, clinical outcomes, response to treatment, and prognosis.[2] Addition of rituximab to cyclophosphamide, doxorubicin, vincristine, and prednisone (R-CHOP) chemotherapy improved the prognosis of DLBCL patients, but more than 30% of DLBCL patients still have a poor prognosis.[3-5] Accordingly, researchers have attempted to discover new treatment approaches for DLBCL to improve outcome.[6]

B-cell lymphoma 2 (Bcl-2) family proteins are key regulators of apoptosis[7] having distinct subgroups that function in complementary ways to retain their original apoptosis regulatory function; antiapoptotic proteins (Bcl-2, Mcl-1, Bcl-w, Bcl-xl, and Bfl-1), proapoptotic effector proteins (Bak and Bax), and pro-apoptotic activator proteins (Bim, Puma, Bid, Bik, Bad, Bmf, Hrk, and Noxa).[8] Several BH3 mimetics that bind to antiapoptotic proteins and trigger cell death are under active clinical development[9]. Among them, Bcl-2 targeting venetoclax has been approved for hematologic malignancies.[10,11] In DLBCL, overexpression of Bcl-2 is one of the factors associated with CHOP resistance.[12,13] Although a recent clinical trial of venetoclax with R-CHOP in Bcl-2+ (by immunohistochemistry) DLBCL patients yielded a promising result,[14] unmet needs still exist regarding the therapeutic use of apoptosis for the following reasons: 1) No effective strategies are present for patients lacking Bcl-2 expression, 2) even in Bcl-2+ patients, resistance to venetoclax occurs easily because of the presence of alternative proteins that retain the antiapoptotic function of Bcl-2 family.[15] Meanwhile, Bfl-1 is the main molecule

that can replace the antiapoptotic function of Bcl-2 in DLBCL, which in turn might be related to both intrinsic and acquired resistance to venetoclax.[16,17] Hence, targeting Bfl-1 is a rational and attractive strategy in DLBCL to improve clinical outcome.

Unfortunately, so far, there are only stapled peptides and early-stage small molecules targeting Bfl-1 and clinically available Bfl-1 inhibitors are not available.[18,19] Considering the difficulty in developing direct Bfl-1 inhibitors, we decided to investigate indirect strategies for inhibiting Bfl-1 at transcriptional and post-translational levels. During Bfl-1 transcription, several transcription factors, including nuclear factor kappa-light-chain-enhancer of activated B cells (NF-kB), retinoid X receptor (RXR), and Wilms' tumor-1 (Wt-1) are involved.[20] Wt-1 directly upregulates Bfl-1 in hematologic malignancies,[21,22] while Noxa is a pro-apoptotic activator protein that closely interacts with Bfl-1.[23] At the post-translational level, Noxa is a counterpart of Bfl-1 and decreases Bfl-1 activity by sequestering activator or effector proteins.[23] Therefore, increased Noxa expression can increase the apoptosis rate. Based on the above evidence and hypothesis, inhibition of histone deacetylase (HDAC), which decreases Wt-1 and increases Noxa levels, was investigated to indirectly regulate Bfl-1. Various HDAC inhibitors were tested and compared to identify the most important HDAC subclass that effectively inhibits Bfl-1. Our study aimed to suggest mechanism-based drug treatment in Bfl-1-high DLBCL patients.

Methods

Cell culture and drugs

DLBCL cell lines (SUDHL-2, OCI-LY-3, RC-K8, TMD-8, OCI-LY-1, and OCI-LY-19) and a kidney cell line HEK 293T were maintained in RPMI-1640, IMDM, alpha MEM and DMEM media supplemented with 10% to 20% heat-inactivated fetal bovine serum (Gibco, NY) and 1% penicillin-streptomycin (Gibco) in a humid environment of 5% at 37 °C. The HDAC inhibitors (panobinostat, trichostatin A, belinostat, and vorinostat) and venetoclax were purchased from Selleck Chemicals. The inhibitors were dissolved in dimethyl sulfoxide (D2650, Sigma Aldrich, St Louis, MO) and stored at -20 °C (-80 °C for long-term storage).

Western blotting

Total protein from cells was isolated using RIPA lysis and extraction buffer (Pierce, Rockford, IL) containing complete protease inhibitor cocktail (Roche) and halt phosphatase inhibitor cocktail (Thermo Fisher Scientific) for 1 h on ice. Equal amounts of protein were loaded on polyacrylamide gels containing SDS, transferred to polyvinylidene fluoride membranes (EMD Millipore, Billerica, MA), and blocked for 1 h using 5% skim-milk (Tech&Innovation, Gang-won, South Korea). Membranes were incubated with primary antibodies overnight, followed by the appropriate secondary antibodies for 1 h. Antibodies used can be found in the supplemental methods. Membranes were stripped using Eastern-Blot Western Blot Stripping Buffer (BioMax, Seoul, South Korea).

Cell proliferation, viability, and apoptosis assay

Cell proliferation was assessed using the Quanti-Max WST-8 Cell Viability Assay Kit (Biomax, Derwood, MD) according to the manufacturer's instructions using a microplate reader (Molecular Devices, San Jose, CA). Cells were seeded in sterile 96-well plates and treated with drugs at increasing concentrations for indicated times. Growth inhibitory concentrations (IC50) of 50% were calculated using GraphPad Prism version 7.0 (GraphPad Software, La Jolla, CA).

Cell viability (the number of live cells to total cells) was determined by trypan blue (0.4%) staining using a Countess II FL automated cell counter (Thermo Fisher Scientific). Experiments were repeated three times independently, and the results are expressed as the mean ± standard deviation (SD).

The ability of HDAC inhibitors and venetoclax to induce apoptosis in cells was measured using the Dead Cell Apoptosis Kit with Annexin V FITC and PI (Thermo Fisher Scientific) and APC annexin V (BD Biosciences, San Jose, CA) according to the manufacturer's instructions. Apoptotic cells were analyzed using BD FACSymphony A3 (BD Biosciences). The results were analyzed using FlowJo 10.7.1 software (Tree Star, Ashland, OR, USA).

Total RNA extraction, cDNA synthesis, and quantitative real-time PCR

Total RNA was isolated from cultured cells using TRIzol reagent (Invitrogen, Carlsbad, CA), and an Epoch Microplate Spectrophotometer (BioTek Instruments, VT) was used to measure RNA concentration. Approximately 1–5 ug of RNA was used to synthesize cDNA using TOPscript RT DryMIX (Enzynomics, Daejeon, South Korea). Real-time PCR was performed using TB Green Premix Ex Taq II (Tli RNaseH Plus) (Takara) on a QuantStudio 1 real-time PCR system (Thermo

Fisher Scientific). *GAPDH* was used to normalize the target mRNA expression. The primer sequences used are listed in Supplemental Figure 1.

Transcriptome Analysis

We performed whole transcriptome sequencing using panobinostat-treated and non-treated SUDHL-2. To identify genes associated with HDAC inhibition, we screened the differentially expressed genes (DEGs) based on Student's t-test. For the functional study, we performed Gene Set Enrichment Analysis (GSEA) using fgsea.[24] We considered the KEGG, GO, hallmark, BioCarta, Reactome, and PID from the predefined Molecular Signatures Database gene set (MsigDB).[25] The result of GSEA was derived as the normalized enrichment score (NES) and its p-value. FDR adjusted P-value < 0.05 was set as the cut-off criteria.

Lentiviral shRNA-mediated Bfl-1 knockdown

The enhanced green fluorescent protein(EGFP) cloning vector was used for lentiviral mediated knockdown. The detailed construction method of the vector can be found in the supplemental methods. The Bfl-1 shRNA or scrambled shRNA plasmids were co-transfected with the lentiviral packaging vectors psPAX2 (from Didier Trono; Addgene plasmid #12260; http://n2t.net/addgene:12260; RRID:Addgene_12260) and pMD2-VSVG (from Didier Trono; Addgene plasmid #12259; http://n2t.net/addgene:12259; RRID:Addgene_12259) into HEK293T cells to produce lentivirus at 37 °C for 48 h. After that, viral supernatant was concentrated using a Lenti-X concentrator (Takara) and added to the cells with 8 ug/mL polybrene (Sigma Aldrich) by the spinoculation method. Infected cells with GFP signals were selected using a FACS-sorting procedure (BD FACSAria II, BD

Biosciences). The sequences used for Bfl-1 inhibition are listed in Supplemental Figure 2 [26,27].

Statistical analysis

Statistical analyses for the efficacy of drugs were performed using GraphPad Prism version 7.0 (GraphPad Software, La Jolla, CA). Data are presented as means ± standard deviation (SD). Multiple comparisons among groups were performed using an analysis of variance (ANOVA). The combination index was calculated using Calcusyn v2.11 (Biosoft, Cambridge, UK).

Results

Bfl-1 expression highly correlates with venetoclax and HDAC inhibitor sensitivity

Six DLBCL cell lines were divided into two groups according to Bfl-1 expression level (Bfl-1+ group: SUDHL-2, OCI-LY-3, TMD-8, and RC-K8, Bfl-1- group: OCI-LY-1 and OCI-LY-19) (Figure 1A-B). Compared to the DLBCL cell lines in the Bfl-1- group, the Bfl-1+ group exhibited reduced sensitivity to venetoclax (Figure 1C). The cell lines in the Bfl-1+ group showed higher IC50 values than those in the Bfl-1- group with venetoclax treatment (Figure 1D). In contrast, Bfl-1+ cell lines were more sensitive to panobinostat, a representative HDAC inhibitor (Figure 1E, Supplemental Figure 3), than Bfl-1- cell lines (Figure 1F). In summary, DLBCL cell lines overexpressing Bfl-1 are sensitive to HDAC inhibitor while insensitive to venetoclax compared to DLBCL cell lines without Bfl-1 expression.

HDAC inhibitors inhibit Bfl-1 by repressing Wt-1 and upregulating Noxa

We hypothesized that the difference in the sensitivity to panobinostat between Bfl-1+/- groups originates from the pharmacological effect of HDACi in downregulating Bfl-1 and Wt-1, and upregulating Noxa. To determine the effect of panobinostat on Wt-1, Noxa, and Bfl-1, we examined the change in the expressions of molecules after panobinostat treatment between the Bfl-1+ group (SUDHL-2, OCI-LY-3) and Bfl-1- group (OCI-LY-19). In the Bfl-1+ group, we could detect decreases in Bfl-1 and Wt-1 levels and increases in Noxa levels in a dose-dependent manner (Figure 2A). This finding was also validated using whole

transcriptome sequencing data of pre- and post-treatment samples (Supplemental Figure 4). In contrast, Noxa was induced at low levels in the Bfl-1- group, and there was no change in Bfl-1 levels despite a reduction in Wt-1 level (Figure 2A). These results were reproduced with other HDAC inhibitors treatment (Supplemental Figure 5A-B). The decrease of Wt-1 and Bfl-1 levels and the increase of Noxa levels were not observed in venetoclax treatment (Figure 2B). Therefore, we could confirm the inhibition of Bfl-1 in Wt-1 and Noxa-dependent manner only with HDAC inhibitors as we have hypothesized.

Then, we confirmed the temporal consequences for reducing Wt-1 and Bfl-1 by assessing the response to the HDAC inhibitor in SUDHL-2. After panobinostat treatment, the decrease in Wt-1 level started from 2 h, which triggered a time-dependent reduction in Bfl-1 level from 6 h (Figure 2C). To reveal the underlying mechanism of Noxa, we analyzed pre- and post-treatment WTS data of SUDHL-2. Via DEG analysis, we found upregulation of the Txnip gene after panobinostat treatment. GSEA revealed that the P53 pathway and cell cycle arrest gene-sets were significantly enriched after panobinostat treatment (Figure 2D-E, Supplemental Figure 6). Txnip increases P53 stability and activity,[28,29] and P53 is a well-known transcription factor of Noxa and induces cell cycle arrest. Therefore, our WTS analysis suggests that the mechanism for Noxa upregulation is closely connected to Txnip and P53.

Altogether, HDAC inhibitors inhibit Bfl-1 at both transcriptional and post-translational levels by suppressing its transcription factor Wt-1 and inducing its antagonist Noxa in DLBCL.

Bfl-1 level is associated with HDAC inhibitor-mediated apoptosis

To clarify that the different sensitivities to HDAC inhibitors and venetoclax are mainly attributable to the difference in apoptosis, we examined the expression levels of apoptogenic factors, including caspase-9, caspase-3, and PARP, in the Bfl-1+/- cells after drug treatment.

When panobinostat was added, SUDHL-2 cells began apoptotic process from 10 nM (Figure 3A), the concentration at which Bfl-1 expression was decreased (Figure 2A). In OCI-LY-3 cells, apoptosis was induced from 30 nM (Figure 3A), the concentration at which Bfl-1 was reduced (Figure 2A). In OCI-LY-19 cells, in contrast, we identified no apoptogenic induction in total form level at broad concentrations (Figure 3A). Contrary to the result of panobinostat, we identified no apparent apoptogenic induction in Bfl-1+ cells with venetoclax treatment. On the contrary, OCI-LY-19 cells underwent apoptogenic induction after venetoclax treatment (Figure 3B).

To confirm the level of apoptosis, we analyzed the apoptotic cells after panobinostat treatment using flow cytometry with annexin V and PI staining. Bfl-1+ cells showed enhanced apoptotic responses (Figure 3C-D). In Bfl-1+ cells, apoptosis rate was significantly increased at the concentration in which Bfl-1 expression was decreased (Figure 2A). Conversely, there was no significant increase in apoptosis rate in OCI-LY-19 cells compared to the previous two cell lines. By analyzing the apoptosis induction at different drug concentrations, we confirmed that panobinostat induces apoptosis by inhibiting Bfl-1, explaining the difference in drug sensitivity between Bfl-1 +/- groups.

Bfl-1 is a critical molecule for deciding cell vulnerability to HDAC inhibitors by inhibiting apoptosis induction

To evaluate the impact of Bfl-1 on cell vulnerability to HDAC inhibitors, Bfl-1 was knocked down in SUDHL-2 cells that have the most robust Bfl-1 expression using a lentiviral infection system. We confirmed the proper infection and Bfl-1 knockdown using several in vitro experiments (Supplemental Figure 7).

Knockdown of Bfl-1 significantly repressed the cell proliferation and development and induced apoptosis in DLBCL (Figure 4A-B). More importantly, we confirmed that panobinostat sensitivity depends on the presence of Bfl-1 (Figure 4C-D). Bfl-1 knockdown cells were insensitive to HDAC inhibitors, which is in contrast to the NI and scrambled vector-transduced cells (Figure 4E, Supplemental Table 1-2). However, a decrease in Wt-1 level in Bfl-1 knockdown cells treated with panobinostat was observed (Supplemental Figure 8), which means that the expression of Wt-1 targets other than Bfl-1 was decreased. Hence, the sensitivity to HDAC inhibitors depends primarily on the presence of Bfl-1.

To examine whether the apoptosis induction by HDAC inhibitor correlates with the baseline Bfl-1 expression levels, we analyzed the apoptogenic factors after panobinostat treatment as previously described. The scrambled vector-transduced cells showed a higher apoptogenic response than Bfl-1 knockdown cells to panobinostat. Interestingly, a significant reduction in Bfl-1 levels in scrambled vector-transduced cells started from 30 nM, different from that in NI cells (10nM) (Figure 5A).

In flow cytometry analysis, only few apoptotic cells were observed even at 30 nM of panobinostat in Bfl-1 knockdown cells (Figure 5B). On the other hand, there was a significant increase in the apoptosis rate at 30 nM (78.2 %) compared to that at 10 nM (20.3%) in scrambled vector-transduced cells, indicating the importance of Bfl-1 in apoptosis induction (Figure 5C). Bfl-1 knockdown cells showed lower apoptosis than scrambled vector-transduced cells following other HDAC inhibitor treatments as well (Supplemental Figure 9A-B). Taken together, we confirm the importance of Bfl-1 in inducing apoptosis following HDAC inhibitor treatment.

Differential sensitivity to HDAC inhibitors in DLBCL suggests a class-specific mechanism of action for Bfl-1 inhibition

Several HDAC inhibitors were used in our study, and the results differed depending on the type of HDAC inhibitors. The most exciting finding is observed with vorinostat, where differential drug sensitivity according to the Bfl-1 expression level was not identified (Figure 6A). Furthermore, no Bfl-1 inhibition following vorinostat treatment was observed (Figure 6B-C), unlike other pan-HDAC inhibitors. Mechanism-wise, vorinostat does not inhibit HDACs in class IIa (4, 5, 7, and 9) [30] unlike panobinostat, trichostatin A, and belinostat. Therefore, we suggest that inhibition of HDAC class IIa can be important to inhibit Bfl-1 in DLBCL.

Discussion

Venetoclax, a highly selective Bcl-2 inhibitor, faces resistance problems when Bcl-2 family antiapoptotic proteins are overexpressed.[31] Among them, Mcl-1 and Bfl-1 have been reported as key determinants for venetoclax efficacy.[32,33] Significant progress has been made in recent years, including the development of Mcl-1 inhibitors.[34] Unlike Mcl-1, several modalities to target Bfl-1 indirectly have been identified, including CDK9, BET inhibitor[15,17] due to the absence of Bfl-1 inhibitor. In this work, we identified another novel approach to inhibit Bfl-1, which is, HDAC inhibitors.

Bfl-1 has been suggested as a promising therapeutic agent to overcome resistance to various drugs such as R-CHOP and venetoclax in blood cancer.[27,32,35] In fact, Bfl-1 is a main antiapoptotic molecule replacing Bcl-2 and Mcl-1 by sequestering pro-apoptotic proteins. After BH3 mimetic exposures, Bfl-1 preserves cell survival while avoiding mitochondrial depolarization.[32] However, the development of the Bfl-1 direct inhibitor has not been successful yet. Some previous studies have reported the indirect inhibition of Bfl-1 through various pharmacological approaches.[15,17] Our study aimed to elucidate a novel method for the indirect inhibition of Bfl-1.

In this study, we confirmed that HDAC inhibitors hamper Bfl-1 at both the transcriptional and post-translational levels in DLBCL and that the sensitivity to HDAC inhibitors depends on the presence of Bfl-1. Furthermore, Bfl-1 knockdown cells showed higher responsiveness to venetoclax than scrambled vector-transduced cells (Supplemental Figure 10A–C), confirming a resistance mechanism

to venetoclax via Bfl-1. At the molecular level, our novel Bfl-1 inhibition approach is based on the biological mechanism, transcription and molecular interaction. Transcriptional changes, including Wt-1 or Txnip, P53 decreases Bfl-1 transcription or increases the transcription of Noxa. Increased Noxa level inhibits antiapoptotic function of Bfl-1 by molecular interaction. To overcome the limitation of using a few cell lines, we additionally validated the association between Bfl-1 expression and panobinostat response using 12 DLBCL cell lines from Cancer Cell Line Encyclopedia (CCLE) and Genomics of Drug Sensitivity in Cancer (GDSC) (Supplemental Figure 11). As a result, we identified that Bfl-1 affects the sensitivity to various drugs, such as HDAC inhibitors and venetoclax.

For clinical application of our study result based on recent molecular classification of DLBCL, we conducted genetic subtyping using sequencing data which is available from CCLE and TCGA, using LymphGen algorithm (Supplemental Table 3-4).[36] Interestingly, 80% of the DLBCL cell lines with high Bfl-1 expression were the MCD subtype and more sensitive to HDAC inhibitors. In the analysis using TCGA data, MCD subtype is the only subtype showing the significant difference in patients' numbers between Bfl-1 high/low group. In the pivotal study, the MCD subtype has higher expression levels of NF-κB target genes than other subtypes,[36] and the association of Bfl-1 and NF-κB in DLBCL has been well documented in the previous studies.[37,38] Although further large-scale studies are needed in the future, we suggest the possibility of using HDAC inhibitors in DLBCL patients with high Bfl-1 expression levels in the MCD group.

Moreover, we identified a synergistic effect of panobinostat combined with lenalidomide in cells with high Bfl-1 expression levels (Supplemental Table 5).

Lenalidomide is a salvage drug in some of relapsed and refractory DLBCL patients. Therefore, we empirically tested whether the combination of lenalidomide with panobinostat is synergistic in the cell line having high Bfl-1 expression. Identifying synergistic partners with HDAC inhibitors may improve clinical outcomes in high Bfl-1 expressing DLBCL.

In conclusion, we have demonstrated that HDAC inhibitors reduce the expression and activity of Bfl-1 in a Wt-1- and Noxa-dependent manner at both the transcriptional and post-translational levels. Additionally, we identified that the sensitivity to HDAC inhibitors is dependent on the presence of Bfl-1 in DLBCL. Because of the absence of BH3 mimetics directly targeting Bfl-1 to date, HDAC inhibitors could provide a new therapeutic option for DLBCL patients using Bfl-1 as a predictive biomarker.

Acknowledgements

This work was supported by the Korea Health Industry Development Institute (KHIDI; grant no. HI14C1277) and National Research Foundation of Korea (NRF; grant no. 2021R1A2C3005360).

Authorship Contributions

EP acquired, analyzed, and interpreted the experimental data and drafted the manuscript. CL performed bioinformatics and statistical analyses. JH, DYS, JMB, YK and SSY devised the study concept and design and JP, JL provided technical guidance for all aspects of the project. All authors discussed the results and contributed to the final manuscript. SSY and YK confirm the authenticity of all the raw data. All authors critically reviewed the manuscript before submission.

Disclosure of Conflicts of Interest

None

References

1. Swerdlow SH, Campo E, Harris NL, et al. *WHO classification of tumours of haematopoietic and lymphoid tissues*. vol 2. International agency for research on cancer Lyon, France; 2008.
2. Rosenwald A, Wright G, Chan WC, et al. The use of molecular profiling to predict survival after chemotherapy for diffuse large-B-cell lymphoma. *New England Journal of Medicine*. 2002;346(25):1937-1947.
3. Coiffier B, Thieblemont C, Van Den Neste E, et al. Long-term outcome of patients in the LNH-98.5 trial, the first randomized study comparing rituximab-CHOP to standard CHOP chemotherapy in DLBCL patients: a study by the Groupe d'Etudes des Lymphomes de l'Adulte. *Blood*. 2010;116(12):2040-2045.
4. Pfreundschuh M, Trümper L, Österborg A, et al. CHOP-like chemotherapy plus rituximab versus CHOP-like chemotherapy alone in young patients with good-prognosis diffuse large-B-cell lymphoma: a randomised controlled trial by the MabThera International Trial (MInT) Group. *The lancet oncology*. 2006;7(5):379-391.
5. Habermann TM, Weller EA, Morrison VA, et al. Rituximab-CHOP versus CHOP alone or with maintenance rituximab in older patients with diffuse large B-cell lymphoma. *Journal of clinical oncology*. 2006;24(19):3121-3127.
6. Wang L, Li L-r, Young KH. New agents and regimens for diffuse large B cell lymphoma. *Journal of Hematology & Oncology*. 2020;13(1):1-23.
7. Ashkenazi A, Fairbrother WJ, Leverson JD, Souers AJ. From basic apoptosis discoveries to advanced selective BCL-2 family inhibitors. *Nature reviews drug discovery*. 2017;16(4):273-284.
8. Cory S, Adams JM. The Bcl2 family: regulators of the cellular life-or-death switch. *Nature Reviews Cancer*. 2002;2(9):647-656.
9. Green DR. A BH3 mimetic for killing cancer cells. *Cell*. 2016;165(7):1560.
10. Liu Y, Mondello P, Erazo T, et al. NOXA genetic amplification or pharmacologic induction primes lymphoma cells to BCL2 inhibitor-induced cell death. *Proceedings of the National Academy of Sciences*. 2018;115(47):12034-12039.
11. D'Aguanno S, Del Bufalo D. Inhibition of anti-apoptotic Bcl-2 proteins in preclinical and clinical studies: Current overview in cancer. *Cells*. 2020;9(5):1287.
12. Gascoyne RD, Adomat SA, Krajewski S, et al. Prognostic significance of Bcl-2 protein expression and Bcl-2 gene rearrangement in diffuse aggressive non-Hodgkin's lymphoma. *Blood, The Journal of the American Society of Hematology*. 1997;90(1):244-251.
13. Tsuyama N, Sakata S, Baba S, et al. BCL2 expression in DLBCL: reappraisal of immunohistochemistry with new criteria for therapeutic biomarker evaluation. *Blood*. 2017;130(4):489-500.
14. Morschhauser F, Feugier P, Flinn IW, et al. A phase 2 study of venetoclax plus R-CHOP as first-line treatment for patients with diffuse large B-cell lymphoma. *Blood, The Journal of the American Society of Hematology*. 2021;137(5):600-609.

15. Boiko S, Proia TA, San Martin M, et al. Targeting Bfl-1 via acute CDK9 inhibition overcomes intrinsic BH3 mimetic resistance in lymphomas. *Blood*. 2020;
16. Yecies D, Carlson NE, Deng J, Letai A. Acquired resistance to ABT-737 in lymphoma cells that up-regulate MCL-1 and BFL-1. *Blood, The Journal of the American Society of Hematology*. 2010;115(16):3304-3313.
17. Esteve-Arenys A, Valero J, Chamorro-Jorganes A, et al. The BET bromodomain inhibitor CPI203 overcomes resistance to ABT-199 (venetoclax) by downregulation of BFL-1/A1 in in vitro and in vivo models of MYC+/BCL2+ double hit lymphoma. *Oncogene*. 2018;37(14):1830-1844.
18. Huhn AJ, Guerra RM, Harvey EP, Bird GH, Walensky LD. Selective covalent targeting of anti-apoptotic BFL-1 by cysteine-reactive stapled peptide inhibitors. *Cell chemical biology*. 2016;23(9):1123-1134.
19. Harvey EP, Hauseman ZJ, Cohen DT, et al. Identification of a covalent molecular inhibitor of anti-apoptotic BFL-1 by disulfide tethering. *Cell chemical biology*. 2020;27(6):647-656. e6.
20. Vogler M. BCL2A1: the underdog in the BCL2 family. *Cell Death & Differentiation*. 2012;19(1):67-74.
21. Simpson LA, Burwell EA, Thompson KA, Shahnaz S, Chen AR, Loeb DM. The antiapoptotic gene A1/BFL1 is a WT1 target gene that mediates granulocytic differentiation and resistance to chemotherapy. *Blood*. 2006;107(12):4695-4702.
22. Ottina E, Tischner D, Herold MJ, Villunger A. A1/Bfl-1 in leukocyte development and cell death. *Experimental cell research*. 2012;318(11):1291-1303.
23. Barile E, Marconi GD, De SK, et al. hBfl-1/hNOXA interaction studies provide new insights on the role of Bfl-1 in cancer cell resistance and for the design of novel anticancer agents. *ACS chemical biology*. 2017;12(2):444-455.
24. Sergushichev AA. An algorithm for fast preranked gene set enrichment analysis using cumulative statistic calculation. *BioRxiv*. 2016:060012.
25. Subramanian A, Tamayo P, Mootha VK, et al. Gene set enrichment analysis: a knowledge-based approach for interpreting genome-wide expression profiles. *Proceedings of the National Academy of Sciences*. 2005;102(43):15545-15550.
26. Merck, Pre-designed shRNA, https://www.sigmaaldrich.com/KR/ko/semi-configurators/shrna?activeLink=selectClones, Accessed 10 October 2020.
27. Brien G, Trescol-Biemont M, Bonnefoy-Berard N. Downregulation of Bfl-1 protein expression sensitizes malignant B cells to apoptosis. *Oncogene*. 2007;26(39):5828-5832.
28. Jung H, Kim MJ, Kim DO, et al. TXNIP maintains the hematopoietic cell pool by switching the function of p53 under oxidative stress. *Cell metabolism*. 2013;18(1):75-85.
29. Suh H-W, Yun S, Song H, et al. TXNIP interacts with hEcd to increase p53 stability and activity. *Biochemical and biophysical research communications*. 2013;438(2):264-269.
30. Marks P, Xu WS. Histone deacetylase inhibitors: Potential in cancer therapy. *Journal of cellular biochemistry*. 2009;107(4):600-608.

31. Yue X, Chen Q, He J. Combination strategies to overcome resistance to the BCL2 inhibitor venetoclax in hematologic malignancies. *Cancer Cell International*. 2020;20(1):1-14.
32. Esteve-Arenys A, Roue G. BFL-1 expression determines the efficacy of venetoclax in MYC+/BCL2+ double hit lymphoma. *Oncoscience*. 2018;5(3-4):59.
33. Prukova D, Andera L, Nahacka Z, et al. Cotargeting of BCL2 with venetoclax and MCL1 with S63845 is synthetically lethal in vivo in relapsed mantle cell lymphoma. *Clinical Cancer Research*. 2019;25(14):4455-4465.
34. Wang H, Guo M, Wei H, Chen Y. Targeting MCL-1 in cancer: current status and perspectives. *Journal of Hematology & Oncology*. 2021;14(1):1-18.
35. Morales AA, Olsson A, Celsing F, Österborg A, Jondal M, Osorio LM. High expression of Bfl-1 contributes to the apoptosis resistant phenotype in B-cell chronic lymphocytic leukemia. *International journal of cancer*. 2005;113(5):730-737.
36. Wright GW, Phelan JD, Coulibaly ZA, et al. A probabilistic classification tool for genetic subtypes of diffuse large B cell lymphoma with therapeutic implications. *Cancer Cell*. 2020;37(4):551-568. e14.
37. Lee C, Song H, Song S, et al. Not BCL2 but BFL1 is overexpressed and have strong correlation with NF-kB pathway in diffuse large B-cell lymphoma. AACR; 2019.
38. Chen L, Monti S, Juszczynski P, et al. SYK inhibition modulates distinct PI3K/AKT-dependent survival pathways and cholesterol biosynthesis in diffuse large B cell lymphomas. *Cancer cell*. 2013;23(6):826-838.

Figure Legends

Figure 1. Bcl-2 family expression in DLBCL and drug sensitivity differences among Bfl-1 +/- cell lines (A) Relative mRNA expression of *Bfl-1*, *Mcl-1*, and *Bcl-2* in DLBCL cell lines. (B) Western blotting for identifying expression levels of Bfl-1, Mcl-1, and Bcl-2 in DLBCL cell lines. (C) Proliferation assay after 72 h from venetoclax treatment using WST-8 in DLBCL cell lines. The proliferation graph representing each group was plotted using the mean value of the proliferation graph of each cell line. (D) Calculated log IC50 values at 72 h after venetoclax treatment. The log IC50 values of Bfl-1+/- groups represent the average log IC50 of each cell line. (E) Proliferation assay after 72 h from panobinostat treatment using WST in DLBCL cell lines. (F) Calculated log IC50 values at 72 h after panobinostat treatment, N/A, could not be determined. **≤ 0.001, ***≤ 0.0001.

Figure 2. Inhibition of Bfl-1 by Wt-1 repression and Noxa overexpression following HDAC inhibitor treatment (A) Wt-1 reduction and Noxa induction following panobinostat treatment. Each cell line is treated with panobinostat for 24 h. (B) No decrease in Wt-1 level and no increase in Noxa level following venetoclax treatment. Each cell line was treated with venetoclax for 24 h. (C) Measurement of Wt-1, Bfl-1, Noxa, Mcl-1, and Bcl-2 protein levels in SUDHL-2 cells at the indicated time points following 30 nM panobinostat treatment. There was no correlation between the reduction in Wt-1 and Mcl-1 level in a time-dependent manner, suggesting that the decrease in Mcl-1 level in Figure 2A is attributable to a mechanism independent of Wt-1 (D) Volcano plot expressing down or upregulated genes after panobinostat treatment for 6 h. (E) Gene set

enrichment analysis results about P53 signaling pathway. Cells were exposed to panobinostat or DMSO for 6 h (n=3).

Figure 3. Identification of apoptosis following panobinostat treatment or venetoclax in Bfl-1 +/- cell lines (A) Identification of the apoptosis pathway following treatment of panobinostat in DLBCL cell lines. Each cell line was treated with panobinostat for 24 h. (B) Identification of the apoptosis pathway following treatment of venetoclax in DLBCL cell lines. Each cell line was treated with venetoclax for 24 h. (C) Induction of apoptosis following treatment of panobinostat in DLBCL cell lines. Each cell line was treated with panobinostat for 24 h. (D) Graph showing the percentage of apoptotic cells in vitro treated with different doses of panobinostat. The number of early apoptotic cells increased at 10 nM but decreased at 30 nM, indicating that the early apoptotic stage cells moved into the late apoptotic stage in SUDHL-2. Error bars indicate S.D for n = 3. *≤ 0.01, ***≤ 0.0001, ns>0.10.

Figure 4. DLBCL cell lines' vulnerability to HDAC inhibitors depends on Bfl-1 (A) Cell proliferation assay on transduced SUDHL-2 cell line. Knockdown of Bfl-1 repressed the proliferation of SUDHL-2. (B) Gene set enrichment analysis results about apoptosis and negative regulation of cell development-related gene-sets. (C) Viability test by trypan blue exclusion assay following 24 h panobinostat treatment. (D) Proliferation assay after 72 h from panobinostat treatment using WST. (E) Calculated log IC50 values at 72 h after panobinostat treatment. * ≤ 0.01, ** ≤ 0.001, *** ≤ 0.0001. Error bars indicate S.D for n = 6 (A and C) or n = 3 (B).

Figure 5. Apoptotic induction by HDAC inhibitor depending on Bfl-1 existence (A) Identification of the apoptogenic molecules following panobinostat treatment between Bfl-1 shRNA and scrambled transduced cells. (B) Analyzed apoptotic cells by Annexin V and PI staining using flow cytometry after panobinostat treatment (0, 10, and 30 nM) for 24 h (C) Graph showing the percentage of apoptotic cells in vitro treated with different doses of panobinostat. Error bars indicate S.D for n = 3. * ≤ 0.05, *** ≤ 0.0001, ns>0.10.

Figure 6. The most important HDACs for Bfl-1 inhibition (A) Proliferation assay after 72 h from vorinostat treatment using WST in transduced cells. (B) No Wt-1, Bfl-1 decrease and Noxa increase after vorinostat treatment in transduced cells. (C) No Wt-1, Bfl-1 decrease and Noxa increase after vorinostat treatment in DLBCL cells.

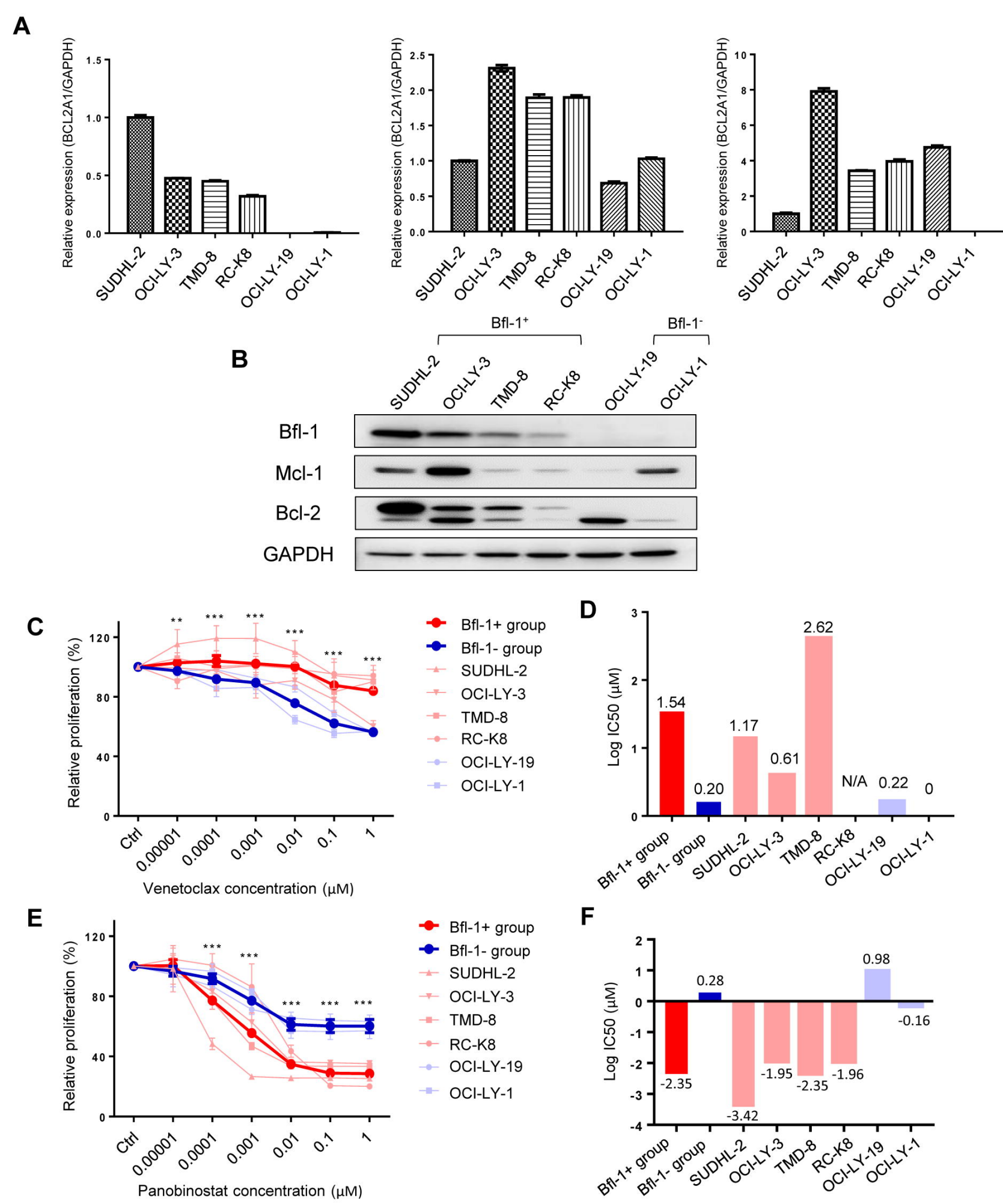
A
Relative expression (BCL2A1/GAPDH)
SUDHL-2
OCI-LY-3
TMD-8
RC-K8
OCI-LY-19
OCI-LY-1
B
Bfl-1+
Bfl-1-
Bfl-1
Mcl-1
Bcl-2
GAPDH
C
Relative proliferation (%)
Venetoclax concentration (μM)
Ctrl
0.00001
0.0001
0.001
0.01
0.1
1
Bfl-1+ group
Bfl-1- group
D
Log IC50 (μM)
1.54
0.20
1.17
0.61
2.62
N/A
0.22
0
E
Panobinostat concentration (μM)
F
-2.35
0.28
-3.42
-1.95
-2.35
-1.96
0.98
-0.16

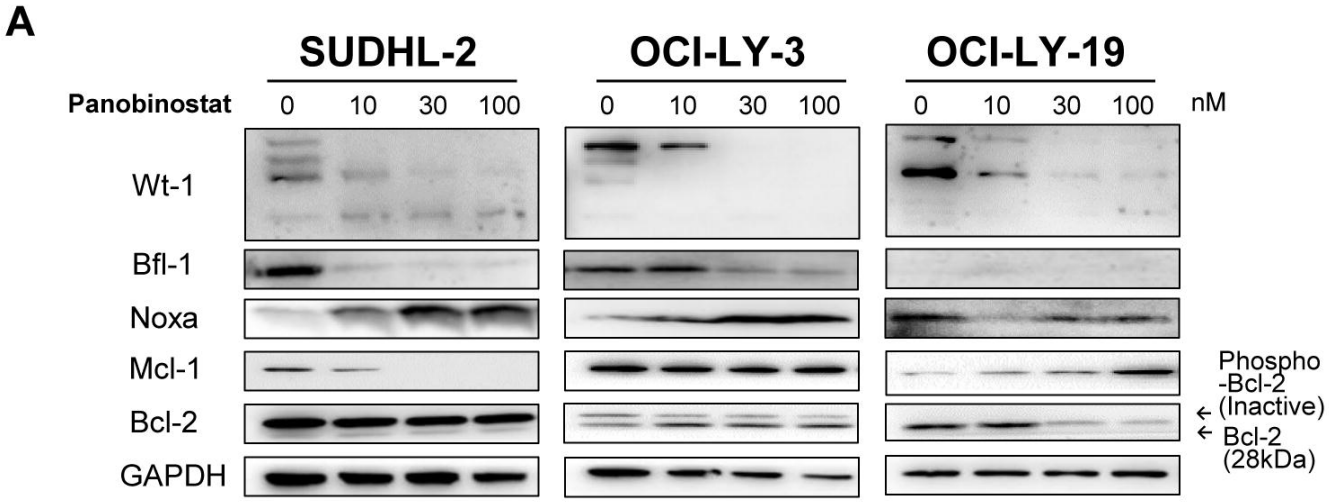
A
SUDHL-2
OCI-LY-3
OCI-LY-19
Panobinostat
0 10 30 100
0 10 30 100
0 10 30 100
nM
Wt-1
Bfl-1
Noxa
Mcl-1
Bcl-2
GAPDH
Phospho -Bcl-2 (Inactive)
Bcl-2 (28kDa)

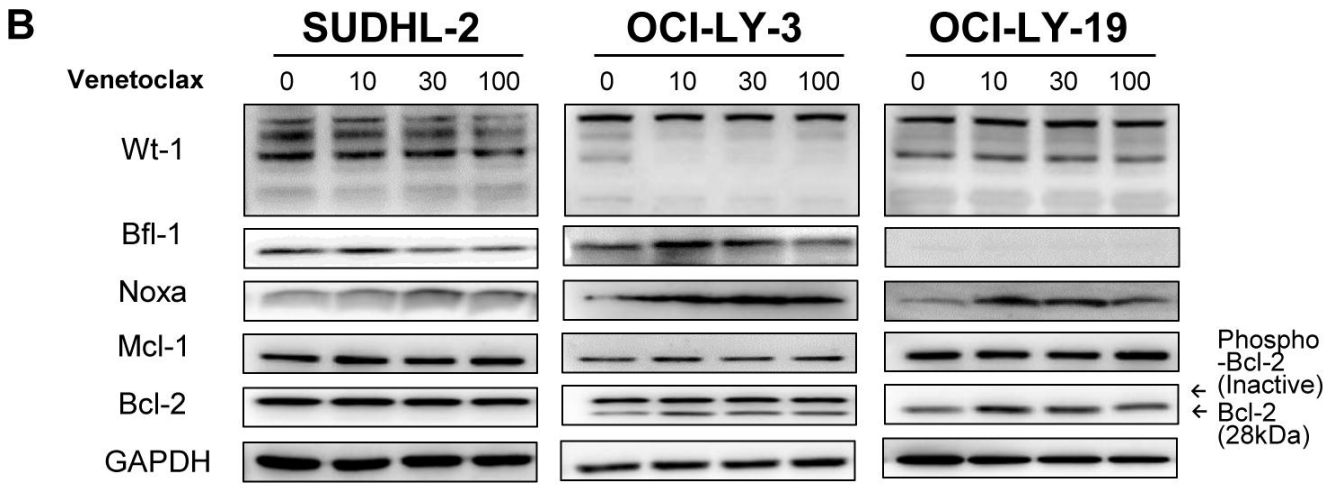
B
SUDHL-2
OCI-LY-3
OCI-LY-19
Venetoclax
0 10 30 100
0 10 30 100
0 10 30 100
Wt-1
Bfl-1
Noxa
Mcl-1
Bcl-2
GAPDH
Phospho -Bcl-2 (Inactive)
Bcl-2 (28kDa)

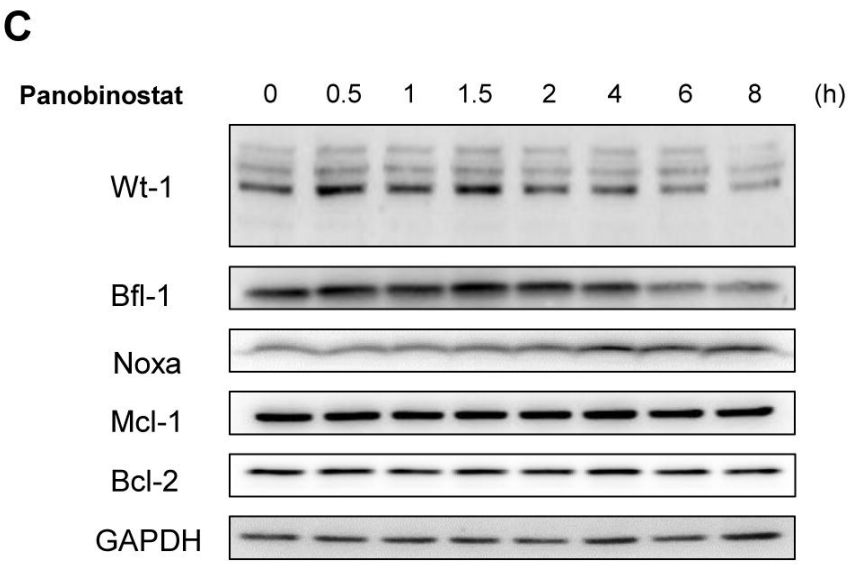
C
Panobinostat
0 0.5 1 1.5 2 4 6 8 (h)
Wt-1
Bfl-1
Noxa
Mcl-1
Bcl-2
GAPDH

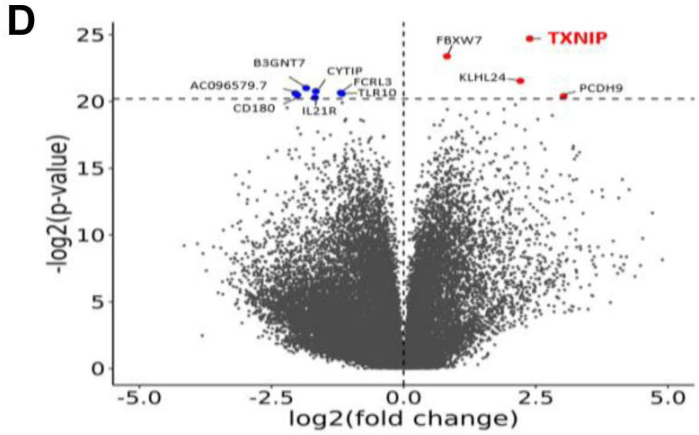
D
TXNIP
FBXW7
KLHL24
PCDH9
B3GNT7
CYTIP
FCRL3
TLR10
AC096579.7
CD180
IL21R
-log2(p-value)
log2(fold change)
25
20
15
10
5
0
-5.0
-2.5
0.0
2.5
5.0

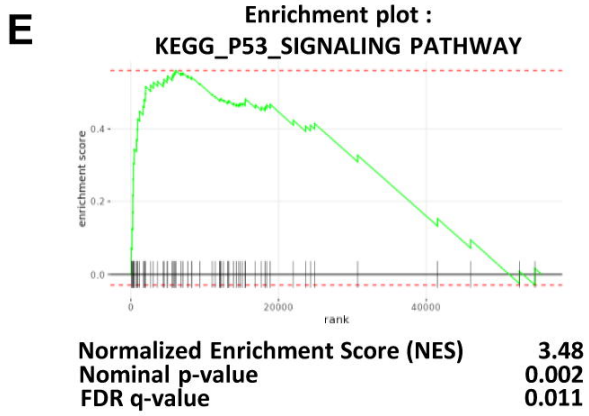
E
Enrichment plot :
KEGG_P53_SIGNALING PATHWAY
enrichment score
rank
0
20000
40000
Normalized Enrichment Score (NES) 3.48
Nominal p-value 0.002
FDR q-value 0.011

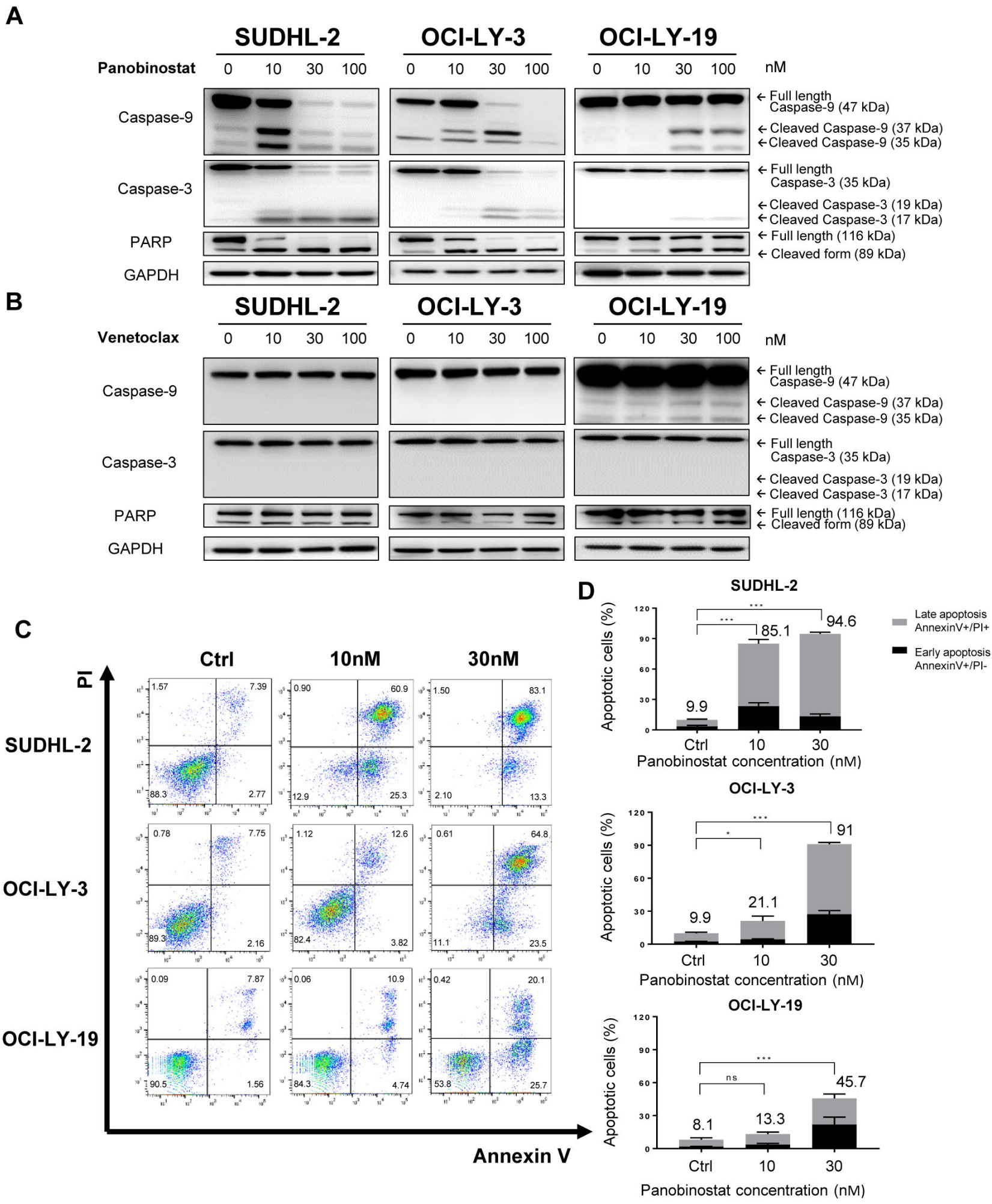
A
SUDHL-2
OCI-LY-3
OCI-LY-19
Panobinostat
0 10 30 100
nM
Caspase-9
Caspase-3
PARP
GAPDH
← Full length Caspase-9 (47 kDa)
← Cleaved Caspase-9 (37 kDa)
← Cleaved Caspase-9 (35 kDa)
← Full length Caspase-3 (35 kDa)
← Cleaved Caspase-3 (19 kDa)
← Cleaved Caspase-3 (17 kDa)
← Full length (116 kDa)
← Cleaved form (89 kDa)
B
Venetoclax
C
Ctrl
10nM
30nM
PI
Annexin V
D
Apoptotic cells (%)
Panobinostat concentration (nM)
Late apoptosis AnnexinV+/PI+
Early apoptosis AnnexinV+/PI-
9.9
85.1
94.6
21.1
91
8.1
13.3
45.7
ns

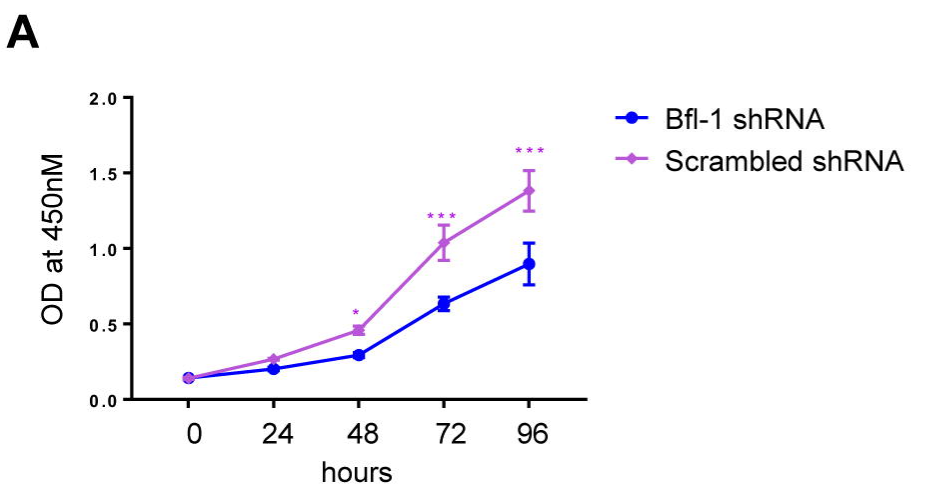
A
OD at 450nM
2.0
1.5
1.0
0.5
0.0
0
24
48
72
96
hours
*
***
***
Bfl-1 shRNA
Scrambled shRNA

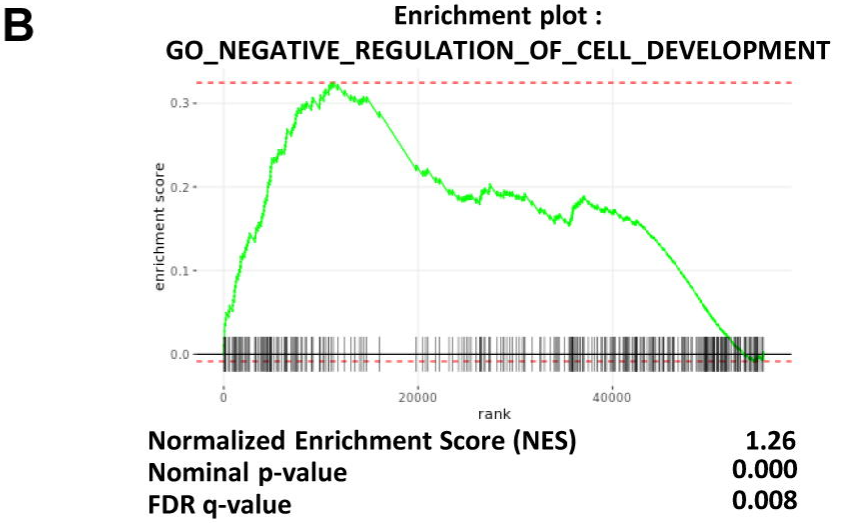
B
Enrichment plot :
GO_NEGATIVE_REGULATION_OF_CELL_DEVELOPMENT
enrichment score
0.3
0.2
0.1
0.0
0
20000
40000
rank
Normalized Enrichment Score (NES) 1.26
Nominal p-value 0.000
FDR q-value 0.008

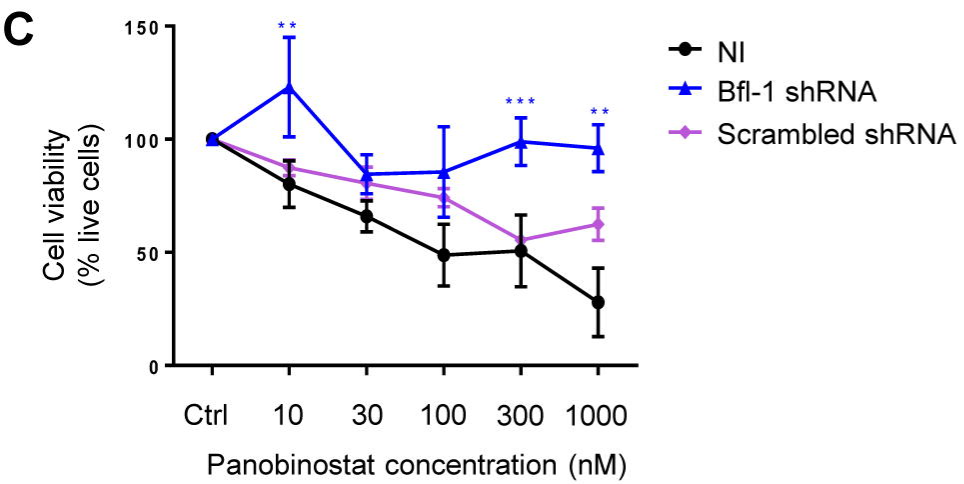
C
Cell viability
(% live cells)
150
100
50
0
Ctrl
10
30
100
300
1000
Panobinostat concentration (nM)
**
***
**
NI
Bfl-1 shRNA
Scrambled shRNA

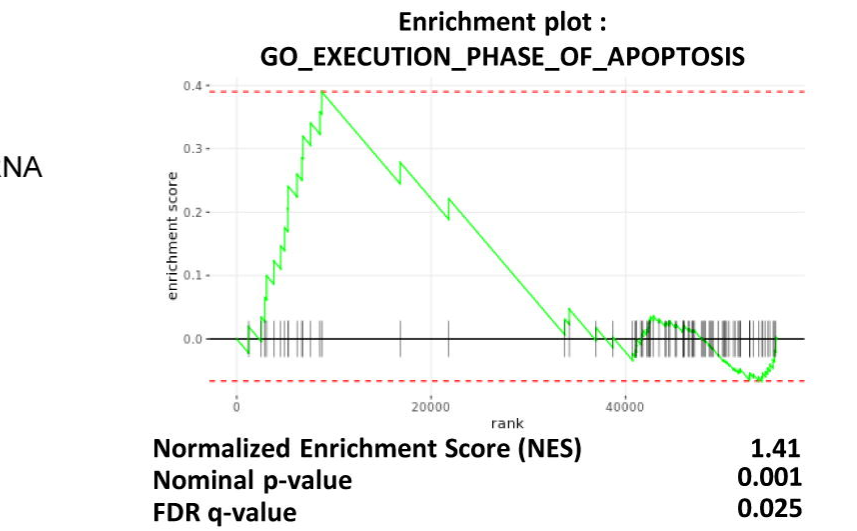
Enrichment plot :
GO_EXECUTION_PHASE_OF_APOPTOSIS
enrichment score
0.4
0.3
0.2
0.1
0.0
0
20000
40000
rank
Normalized Enrichment Score (NES) 1.41
Nominal p-value 0.001
FDR q-value 0.025

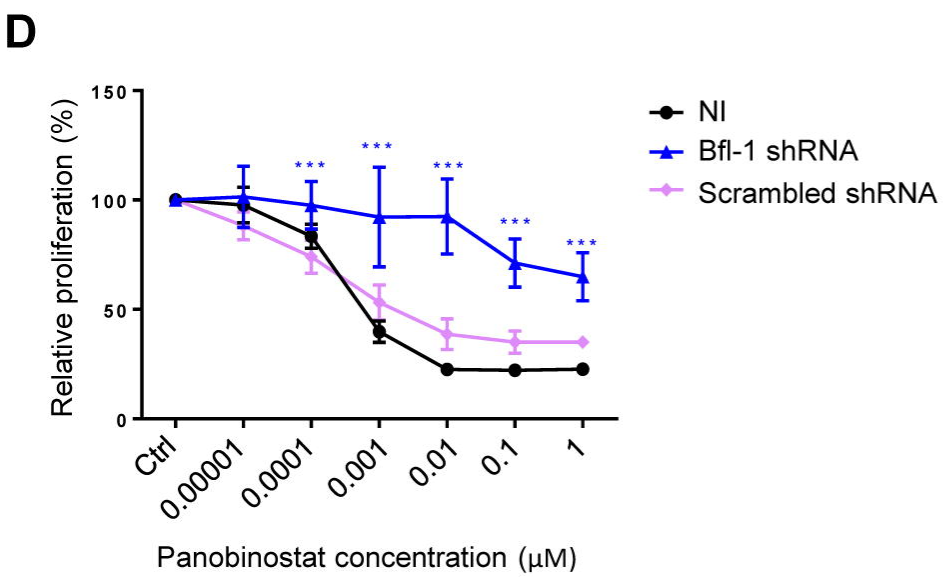
D
Relative proliferation (%)
150
100
50
0
Ctrl
0.00001
0.0001
0.001
0.01
0.1
1
Panobinostat concentration (µM)
***
***
***
***
***
NI
Bfl-1 shRNA
Scrambled shRNA

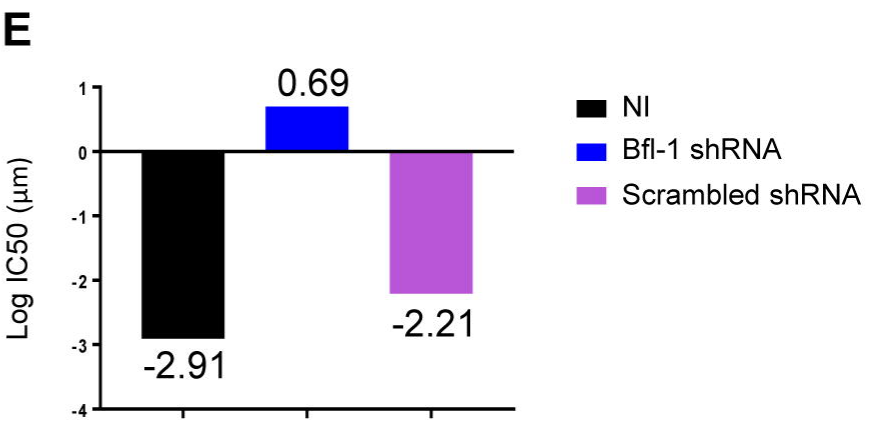
E
Log IC50 (µm)
1
0
-1
-2
-3
-4
0.69
-2.91
-2.21
NI
Bfl-1 shRNA
Scrambled shRNA

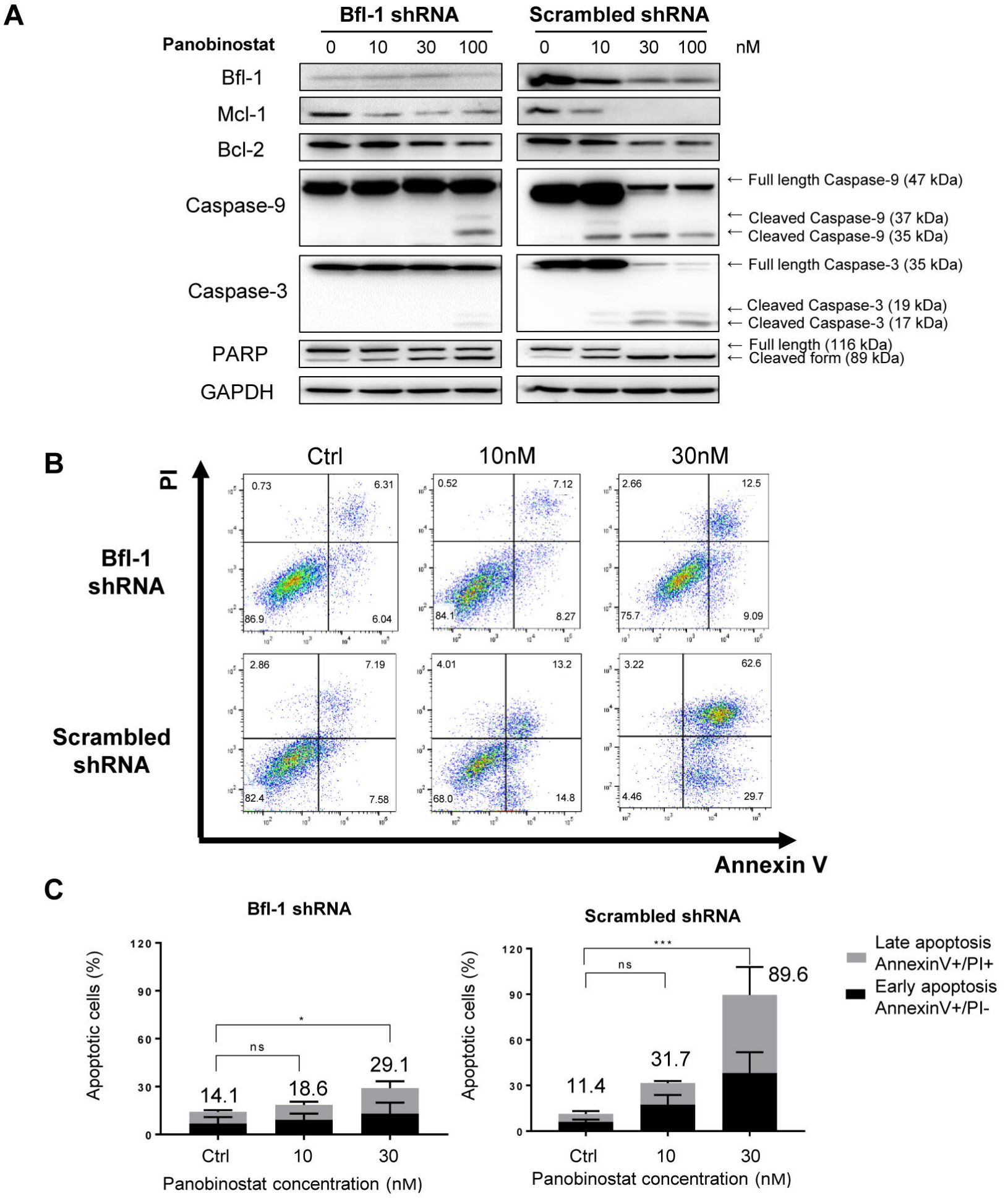
A
Bfl-1 shRNA
Scrambled shRNA
Panobinostat
0 10 30 100
0 10 30 100 nM
Bfl-1
Mcl-1
Bcl-2
Caspase-9
Caspase-3
PARP
GAPDH
← Full length Caspase-9 (47 kDa)
← Cleaved Caspase-9 (37 kDa)
← Cleaved Caspase-9 (35 kDa)
← Full length Caspase-3 (35 kDa)
← Cleaved Caspase-3 (19 kDa)
← Cleaved Caspase-3 (17 kDa)
← Full length (116 kDa)
← Cleaved form (89 kDa)
B
Ctrl
10nM
30nM
PI
Bfl-1 shRNA
Scrambled shRNA
Annexin V
0.73
6.31
86.9
6.04
0.52
7.12
84.1
8.27
2.66
12.5
75.7
9.09
2.86
7.19
82.4
7.58
4.01
13.2
68.0
14.8
3.22
62.6
4.46
29.7
C
Bfl-1 shRNA
Scrambled shRNA
Apoptotic cells (%)
120
90
60
30
0
ns
*
***
14.1
18.6
29.1
11.4
31.7
89.6
Ctrl
10
30
Panobinostat concentration (nM)
Late apoptosis
AnnexinV+/PI+
Early apoptosis
AnnexinV+/PI-

A

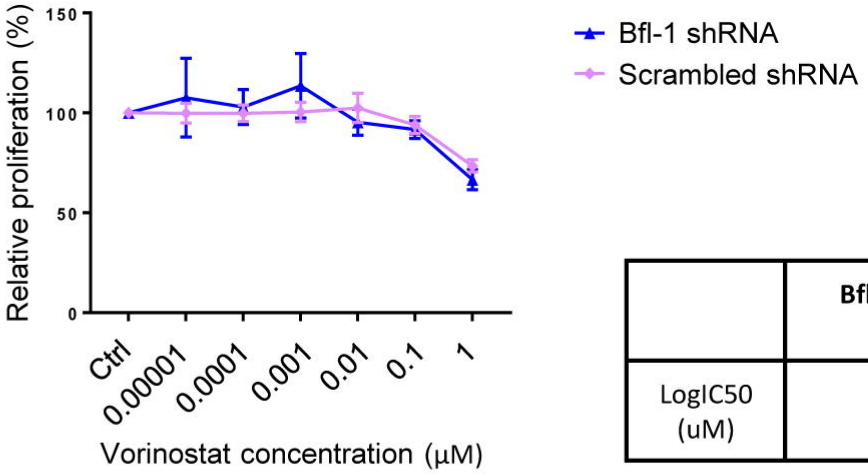

	Bfl-1 shRNA	Scrambled shRNA
LogIC50 (uM)	0.389	0.523

B

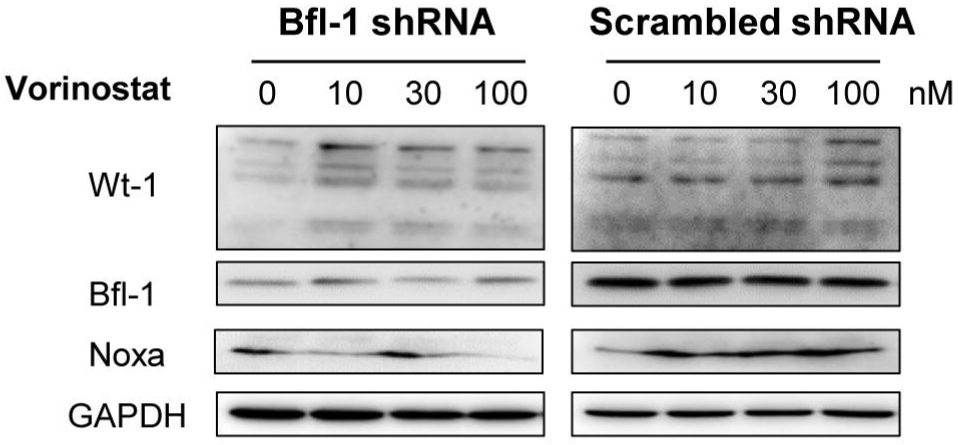
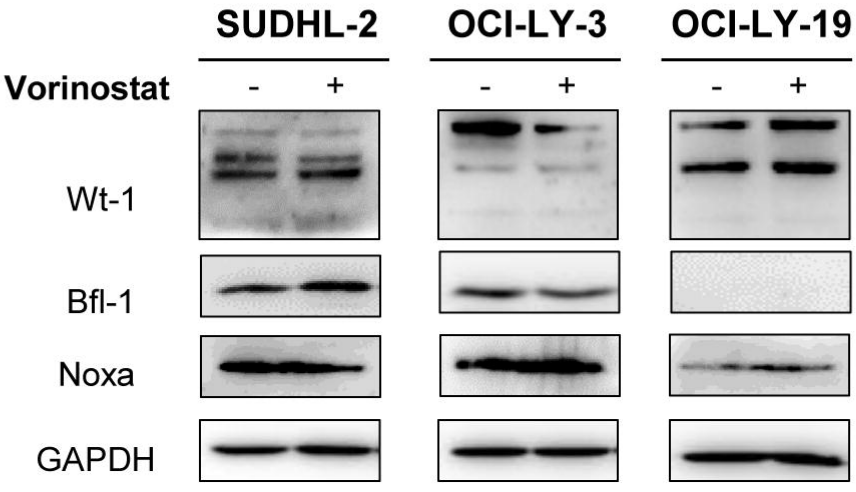
C